IEEE Access
Multidisciplinary ⋮ Rapid Review ⋮ Open Access Journal

Received July 27, 2020, accepted August 8, 2020, date of publication August 13, 2020, date of current version August 27, 2020.

Digital Object Identifier 10.1109/ACCESS.2020.3016432

A Low-Profile Hybrid Multi-Permittivity Dielectric Resonator Antenna With Perforated Structure for Ku and K Band Applications

IHSAN AHMAD ZUBIR[1], MOHAMADARIFF OTHMAN[2], UBAID ULLAH[3], (Member, IEEE), SHAHANAWAZ KAMAL[1], MOHD FARIZ AB RAHMAN[4], ROSLINA HUSSIN[1], MOHAMAD FAIZ BIN MOHAMED OMAR[5], ABDULLAHI S. B. MOHAMMED[1], MOHD FADZIL BIN AIN[1,5], ZAINAL ARIFIN AHMAD[6], AND MOHD ZAID ABDULLAH[1], (Member, IEEE)

[1]School of Electrical and Electronic Engineering, Universiti Sains Malaysia, Nibong Tebal 14300, Malaysia
[2]Department of Electrical Engineering, University of Malaya, Kuala Lumpur 50603, Malaysia
[3]Networks and Communication Engineering Department, Al Ain University of Science and Technology, Abu Dhabi, United Arab Emirates
[4]Faculty of Bioengineering and Technology, Universiti Malaysia Kelantan, Jeli 17600, Malaysia
[5]Collaborative Microelectronic Design Excellence Centre, Sains@USM, Bayan Lepas 11900, Malaysia
[6]School of Materials and Mineral Resources Engineering, Universiti Sains Malaysia, Nibong Tebal 14300, Malaysia

Corresponding author: Mohd Fadzil Bin Ain (eemfadzil@usm.my)

This work was supported by the Ministry of Higher Education, Malaysia, underthe Fundamental Research Grant Scheme 203.PELECT.6071429.

ABSTRACT A wideband hybrid dielectric resonator antenna (DRA) consisting of a rectangular slot patch and a perforated stacked cylindrical dielectric resonator (DR) is proposed. A rectangular slot was etched on the grounding side of a microwave laminate ($\epsilon_s = 3.38$) to excite the hybrid resonator at a high frequency. The stacked DR used consists of three different layers of permittivity, in which air-cavity was introduced internally to form a perforated structure. With a proper stacking arrangement of the perforated DRs on top of the rectangular slot, their operating frequencies were merged together to produce a wideband hybrid DRA. It was found that the combination of the stacked DR with perforated structure in the hybrid element had yielded an impedance bandwidth of as wide as 75.8% (12.2 GHz - 27.1 GHz). Huge improvement in bandwidth was successfully achieved in this study in comparison to that without a perforated structure of only 48.9%. Simulation of the antenna was performed in time domain using Computer Simulation Technology (CST) and was subsequently verified with the measurement results. The average simulated and measured directivity of the antenna were recorded to be 6.05 dBi and 5.65 dBi, respectively, with a stable broadside radiation throughout the operating range of frequency. The radiation characteristics were seen to be broadside in both the E-plane and H-plane.

INDEX TERMS Wideband, hybrid dielectric resonator, perforated structure, Ku band, K band, cylindrical DR, rectangular slot patch.

I. INTRODUCTION

Dielectric resonator antenna (DRA) had been developed and introduced by Long *et al.* [1]. Following this, DRA is receiving an extensive attention owing to its intrinsic advantages. These include its compact size, high radiation efficiency, light weight and variety of feeding mechanisms [2], [3]. Bandwidth enhancement in a DRA design is a major consideration for many practical applications. Various techniques had been proposed to improve the bandwidth of DRAs, for instance, the uses of dielectric resonators (DRs) with different layers of dielectric material [4], parasitic slot [5] and special DR geometries [6]. Besides, modification in the structure of DRs can also be exploited to improve the impedance bandwidth of DRA [7]. Perforation technique through a combination of a number of holes and diameter was applied by [8] to improve the bandwidth of a cylindrical DRA to 26.7%. More considerable improvement in bandwidth of 56% was achieved by [9]

The associate editor coordinating the review of this manuscript and approving it for publication was Chan Hwang See.

This work is licensed under a Creative Commons Attribution 4.0 License. For more information, see https://creativecommons.org/licenses/by/4.0/

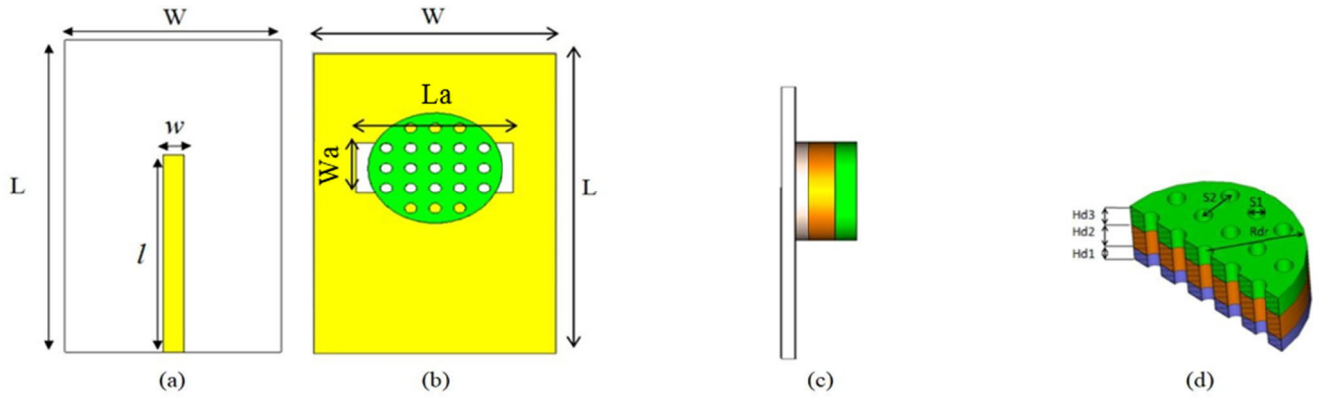

FIGURE 1. Geometry of the hybrid DRA (a) Front view (b) Back view (c) Side view (d) Isometric view.

through the use of a perforated rectangular DRA integrating with radiating probe feeder. Another proposed technique to broaden the bandwidth of an antenna represents the use of hybrid structure which can be considered as the combination of two different radiating resonator elements [10]–[18]. Ultra-wideband characteristics of a high-frequency antenna were obtained in the study by [10] by creating a high-profile antenna with a monopole protruding from the ring-shaped resonators. Most of the previous studies on the hybrid antenna involved either altering the structure of the ground plane or the feeding mechanism to generate additional resonance modes and circularly polarized antenna. As a matter of fact, this method involves a complex feeding design as shown by [11] with a modified cross-slot and trapezoidal patch line as studied by [13]. Dual C-shaped microstrip line was used in the studies by [14] to excite DR and simultaneously perform as the radiating source. Tri-band hybrid antenna with circular shape and cylindrical DR incorporation was proposed by [16] for MIMO application with a maximum bandwidth of 51.21%. The same author reported on the use of a ring DR with a stepped slot to achieve 85.21% impedance bandwidth for similar application [17]. In addition, a study utilizing water as DR for a hybrid antenna operating at a very low frequency ranging from 69 to 171 MHz was also reported [18].

Several studies have been carried out in depth for the dielectric resonator antennas. However, as of today, there is still a lack of significant studies conducted on the wideband characteristic of a hybrid antenna. This includes an optimization on stacked DR configuration with different dielectric substrates incorporation as well as the perforated structure. In the studies by [9], similar work on the wideband hybrid antenna was reported which was using perforated rectangular DR with probe coupling which simultaneously acted as an antenna. However, the stacked rectangular DR became bulky when using a single dielectric material of a permittivity of 10.2. Similar bulky issues arose in studies conducted by [14] in which two identical solid DRs with two-layer structure were used. Stacked DR was also used in the work done by [13] using layers of similar dielectric substrate without stacked optimization.

Therefore, to acquire a wideband response, stacked cylindrical DR using various dielectric substrates and perforation technique was emphasized. A stacked structure consists of a combination of three distinct layers of cylindrical DR placed on a resonating slot of a grounded dielectric substrate. The antenna was designed to resonate with a wide impedance bandwidth by optimizing the stack order of DRs, the permittivity of DRs and the dimension of the resonating slot. The slot coupling is used as a feeder to suit high-frequency applications and to prevent any radiating effect of microstrip line to DR [3]. The impedance bandwidth of the antenna was further improved by perforating the stacked DRs. By performing a comprehensive parametric analysis on different parameters, the resonances obtained from the three stacked layers and the slot were merged together. For comparison, the proposed antenna was compared with the currently published state of the art designs. A summary of wideband hybrid DRAs is listed in Table 1, in which the antennas are compared in terms of electrical size, impedance bandwidth and radiation efficiency. Following this, the antenna design and its details are described in Section 2 while the experimental results and analysis are provided in Sections 3 and 4, respectively.

II. ANTENNA DESIGN

The structure of the proposed wideband hybrid DRA is shown in Figure 1. This antenna consists of three stacked DRs loaded on top of a resonating slot etched on the ground plane of RT/Duroid RO4003C substrate ($\epsilon_r = 3.38$) with a thickness of 0.813 mm. The width W, length, L and thickness of the dielectric substrate are 20 mm, 30 mm and 0.813 mm, respectively. In this design, three different dielectric substrates which are RO4003C ($\epsilon_r = 3.38$) with a thickness of 0.813 mm, FR-4 ($\epsilon_r = 4.55$) with a thickness of 1.6 mm and RT/Duriod 6010 ($\epsilon_r = 10.2$) with a thickness of 1.27 mm were used as the resonating elements. Each resonator has a radius, R_{dr} of 5.5 mm. With respect to the resonating rectangular slot on the ground plane, the resonators were stacked in an increasing value of permittivity from bottom to top. In order to isolate the resonators from any unwanted coupling or spurious radiation from the feeder, the resonators

were placed on a slot that was etched on the ground plane. The microstrip transmission line excites the slot (aperture) by forming a standing-wave with its maximum current located at the end of the microstrip line and also at the center of the slot. Simulation of the antenna was performed using the Computer Simulation Technology (CST) in time domain and the results were then validated experimentally.

A. ESTIMATION OF APERTURE SLOT LENGTH AND WIDTH

The slot length and width affect the coupling level [23], bandwidth [24] and the back-radiation level [25]. In order to have maximum coupling, the dielectric should be centered over the slot. Whereas, the open end of feed line is positioned at the center of the slot which have strongest current distribution and have strong magnetic coupling. In this configuration, the dominant mechanism for this coupling is magnetic polarization. In order to have a good front to back ratio (F/B ratio), the size of the rectangular slot should be chosen precisely as the slot dimensions control the value of coupling between the feed line and the resonator. With a small area of rectangular slot, the efficiency of the antenna is improved due to lower back radiation level [26]. The length of rectangular slot, L_a can be determined by Equation (1) while the width W_a of the slot is calculated by Equation (3) [27],

$$L_a = \lambda_g \tag{1}$$

$$\lambda_g = \frac{\lambda_o}{\sqrt{\epsilon_{eff}}} \tag{2}$$

$$W_a = \frac{\lambda_o}{4} \tag{3}$$

where, λ_o is the wavelength of center frequency at 18 GHz, and ϵ_{eff} is the effective permittivity of the stacked resonator and the substrate.

B. DESIGN OF STACKED PERFORATED DIELECTRIC RESONATOR ANTENNA (SPDRA)

In this design, three layers stacked dielectric materials with different permittivity were used. In theory, DRA must be fabricated from a high dielectric constant material to achieve a strong electromagnetic coupling between the source and the resonator. On the other hand, to operate the DRAs over a wide bandwidth, the DRAs must have a low dielectric constant. These three different permittivity cylindrical dielectric resonators were stacked in the order of their permittivity to achieve wide bandwidth antenna is proposed. The lowest permittivity, $\epsilon_{r1} = 3.38$ (DR1) dielectric pellet was loaded directly on top of resonating slot, followed by medium permittivity, $\epsilon_{r2} = 4.55$ (DR2) and high permittivity dielectric resonators, $\epsilon_{r3} = 10.2$ (DR3). However, the input impedance of the structure does not match enough and need to be improved further to enhance the bandwidth of the antenna. The cylindrical stacked DRs is drilled using CNC machine to introduce air inside the DRs as shown in Figure 2. The existence of air will reduce the effective permittivity of the DRs and improve the bandwidth of the antenna.

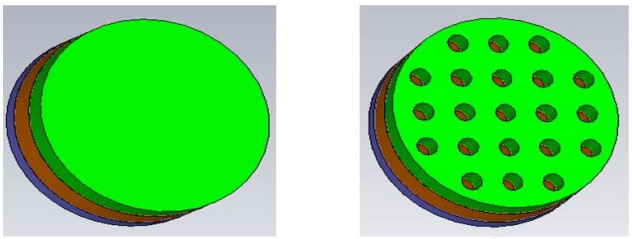

FIGURE 2. Isometric view. (a) Solid cylindrical stacked DRs (b) Perforated stacked DRs.

C. DETERMINATION OF THE DIAMETER OF STACKED CYLINDRICAL DR_S

The diameter, d of stacked DRs can be determined using Equation (4). The stacked DRs are made from the standard dielectric material of available substrates in, RT/Duroid 4003 with the permittivity $\epsilon_{r1} = 3.38$ and thickness $H_{d1} = 0.813$ mm, FR4 with permittivity $\epsilon_{r2} = 4.55$ and thickness $H_{d2} = 1.6$ mm and RT/Duroid 6010 with the permittivity $\epsilon_{r3} = 10.2$ and thickness $H_{d1} = 1.27$ mm. The calculation of the diameter also considers the permittivity of substrate $\epsilon_s = 3.38$ with the thickness $H_s = 0.813$ mm. Hence, the diameter of DRs obtained using Equation (4) is around 11 mm with desired resonant frequency, $f_0 = 18$ GHz.

$$f_o = \frac{2.208 \times c}{2\pi h\sqrt{\epsilon_{eff}+1}}[x] \tag{4}$$

$$x = \left[1 + 0.7013\left(\frac{r}{H_{eff}}\right) - 0.002713\left(\frac{r}{H_{eff}}\right)^2\right] \tag{5}$$

$$H_{eff} = H_{d1} + H_{d2} + H_{d3} + H_s \tag{6}$$

D. PERFORATED STACKED CYLINDRICAL DR_S STRUCTURE

Referring to (7), as the value of permittivity increases, the quality factor, $Q - factor$ also increases [28]. This results in more electrical and magnetic energies being confined inside the DRs. In the proposed design, the total effective permittivity of DR, ϵ_{eff} was reduced by creating air cavities inside the resonator. Consequently, more electrical and magnetic energies will quickly dissipate in the form of resonance. Instead of storing energy, DR tends to radiate more power, thus improving the impedance bandwidth at the expense of decreasing $Q - factor$.

$$Q = 2\omega_{eff}\frac{Stored\ Energy}{Radiated\ Power}\alpha 2\omega_o\left(\epsilon_{eff}\right)^p\left(\frac{Volume}{Surface}\right)^s \quad with;\ p > s \geq 1 \tag{7}$$

The creation of holes in DRs is generally known as perforation, which is one of the techniques used to reduce the $Q-factor$ of a DR [8], [29], [30]. Holes were drilled through the DR in a uniform lattice arrangement. The presence of these holes in turn introduced air permittivity into the resonator. For a uniform effective permittivity of the DR to be achieved, the lattice spacing and hole diameter were kept under one half of the guided wavelength at 18 GHz. The effective permittivity, ϵ_{eff} of DR is approximately determined

TABLE 1. Summary of various wideband DRAs.

Hybrid Mechanism	Height	Electrical Area	Center Freq.	Rad. Eff.	Bandwidth	Reference
Half split cylindrical DR	0.161 λ	9.42 λ^2	4.50 GHz	-	63.7%	[19]
Three-element cylindrical DR	0.159 λ	48.48 λ^2	4.42 GHz	-	52.9%	[20]
Four-element cylindrical DR	0.145 λ	78.66 λ^2	4.03 GHz	-	58.1%	[21]
Rectangular DR + perforation	0.145 λ	9.03 λ^2	2.82 GHz	> 85%	56.0%	[22]
Rectangular slot + perforated + cylindrical DR	0.24 λ	2.57 λ^2	19.65 GHz	90.3%	75.8%	Proposed

by the average volumetric of air present inside the holes and the dielectric material.

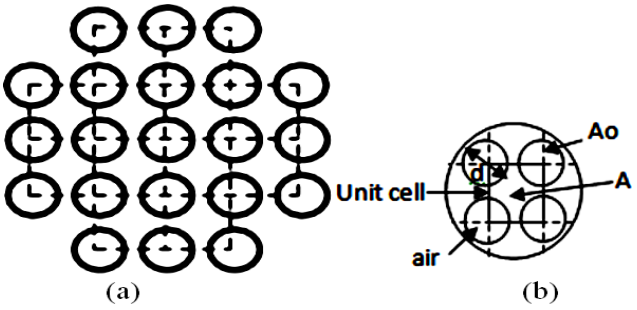

FIGURE 3. Perforated DR with square lattice (a) Full unit cells of lattices (b) A unit cell of lattice.

In this proposed design, ϵ_s was calculated using a modified form of static capacitance model, in which the filling factor, α of the perforated DR was also considered. The lattice was arranged in a square form as shown in Fig. 3(b). The calculation of α is given in (8),

$$\alpha = \frac{A_o}{2A} \tag{8}$$

where, A_o is the area of the hole and A is area of the unit cell.

After simplification, of α a square lattice is determined from (9):

$$\alpha = \frac{\pi d^2/4}{s^2} = \frac{\pi}{4}\left(\frac{d}{s}\right)^2 \tag{9}$$

where, s is the distance between two holes (2 mm). Given the diameter of the hole, d to be 1 mm, the calculated α was 0.1963. To predict the ϵ_{perf} of the perforated stacked DR, the following (10) was used, where ϵ_{sol} is the effective permittivity of the solid stacked DR (without holes) which can be calculated using the original static capacitance model shown in (11).

$$\epsilon_{perf} = \epsilon_{sol}\,(1-\alpha) + \alpha \tag{10}$$

$$\epsilon_{sol} = \left[\frac{H_{stack}}{\left(H_{d1}/\epsilon_{r1}\right) + \left(H_{d2}/\epsilon_{r2}\right) + \left(H_{d3}/\epsilon_{r3}\right)}\right] \tag{11}$$

H_{d1}, H_{d2}, H_{d3}, and H_{stack} are the heights of DR_1, DR_2, DR_3 and the stacked DR_s, respectively. The value of ϵ_{sol} was 5.14 and reduced to 4.33 for ϵ_{perf}. In order to include the effect of dielectric substrate on DRA, the original static capacitance model was again applied to calculate the ϵ_{eff} of the overall DRA. From (12), the value of ϵ_{eff} was 4.12, where H_{eff} is the total height of DRA (dielectric substrate and stacked), and H_s and ϵ_s are the height and permittivity of the substrate, respectively.

$$\epsilon_{eff} = \left[\frac{H_{eff}}{\left(H_s/\epsilon_s\right) + \left(H_{stack}/\epsilon_{perf}\right)}\right] \tag{12}$$

Equation (10) shows that by introducing perforation, the value of permittivity of DR reduced from 5.14 to 4.33. From (7), it was proven that via perforation, the $Q-factor$ was reduced and thus enhancing the bandwidth of the DRA.

III. ANTENNA ANALYSIS

In this section, a detailed analysis on the parameters influencing the performance of the proposed hybrid antenna in terms of impedance bandwidth, compactness and electromagnetic coupling to the source are discussed. The analysis focused on several parameters including stack order, slot dimensions and number of holes drilled in the dielectric resonator. All the parametric analyses were performed using CST.

A. DIELECTRIC RESONATORS ARRANGEMENT

In order to optimize the proposed design of hybrid DRA, different stack orders of the cylindrical DR with constant radius were simulated. Three dielectric resonators of different materials with permittivity of $\epsilon_1 = 3.38$, $\epsilon_2 = 4.55$ and $\epsilon_3 = 10.2$ were properly stacked, producing a wideband operation. The simulated reflection coefficient with different stack order is presented in Fig. 4. The bottom layer of the stacked DR was fixed while the other layers on top were varied. It can be observed that the bandwidth of the hybrid DRA was greatly influenced by the DR arrangement. Table 2 gives the overview on the bandwidth of the DRA for different stack arrangements. All the DR arrangements depicted a dual band operation with the highest bandwidth of 48.4% was generated when ϵ_1 was placed at the bottom followed by ϵ_2 and ϵ_3. Thus, in order to merge all the frequency resonances and to form a wideband antenna, the most appropriate stack arrangement of the DR from bottom to top was in the order of ϵ_1, ϵ_2 and ϵ_3.

B. SLOT DIMENSIONS

As stated in the previous section, the proposed DRA was made excited using a rectangular slot etched on the ground plane. A microstrip line which was placed on top of the grounded substrate was used to excite the aperture acting as the resonating slot. The DR was placed on top of the slot in

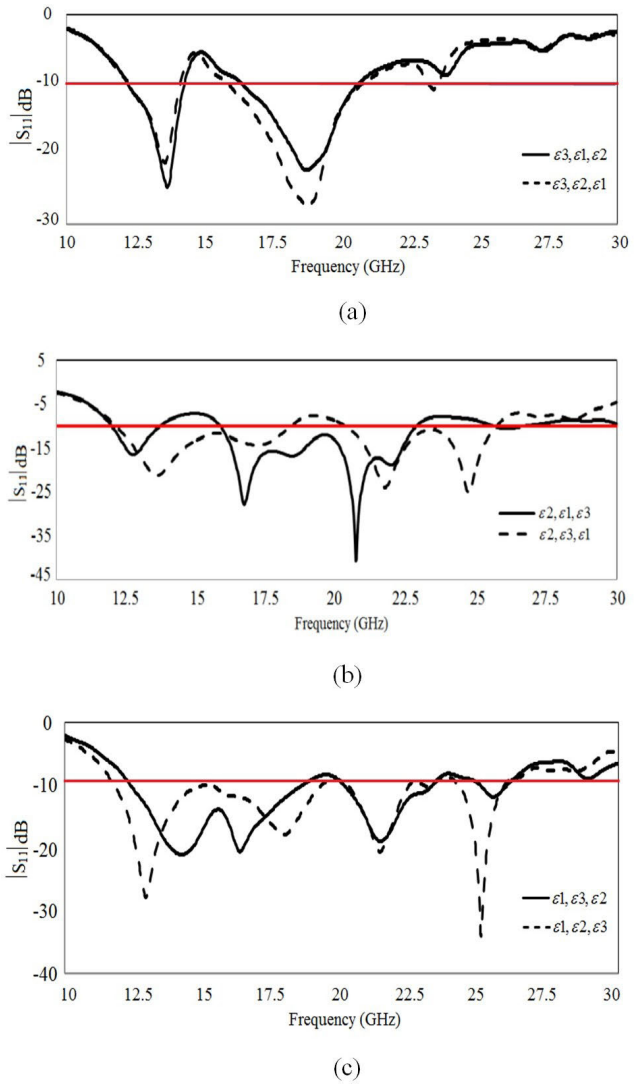

FIGURE 4. Simulated reflection coefficient of wideband DRA (a) Fixed bottom placement of DR layer, ϵ_3 (RO4003C) (b) ϵ_2 (FR4) (c) ϵ_1 (Duriod 6010).

TABLE 2. Bandwidth comparison between different stack arrangements of the dielectric resonator.

Bottom of Stack	Middle of Stack	Top of Stack	Maximum Bandwidth (%)
10.2	3.38	4.55	30.1
10.2	4.55	3.38	33.3
4.55	10.2	3.38	36.8
4.55	3.38	10.2	36.5
3.38	10.2	4.55	46.2
3.38	4.55	10.2	48.4

a way that maximum energy was coupled from the slot to the dielectric resonator. The slot width, W_a and length, L_a are the important parameters to be considered to achieve an impedance matching over a wide bandwidth.

Fig. 5 shows the simulated reflection coefficient of DRA with different slot lengths, L_a ranging from 9 mm to 17 mm with 2 mm step size. It was clearly indicated that L_a affected

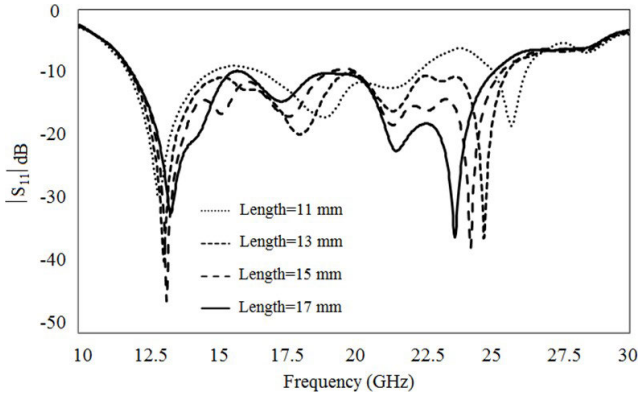

FIGURE 5. Simulated reflection coefficient of the wideband DRA with different values of slot length.

the resonant frequency and impedance matching of the antenna. Referring to the response of the reflection coefficient, it is also exhibited that the optimal dimension of the rectangular slot should be kept at $\lambda/4$ of 18 GHz where $W_a = 5$ mm and $L_a = 13$ mm. This is to maintain a wide impedance bandwidth in the desired frequency range. There were four resonances in the frequency response of the DRA emerging from the combination of a stacked resonator and a resonating slot. These resonances were merged together to form a wideband DRA. The first three resonances were not affected by the variation of the slot dimension except for the impedance matching across the operating band. This indicated that the resonances were specifically sensitive to the stacked DR with permittivity of 3.38, followed by 4.55 and 10.2. However, the last resonance started to move downward when the slot size was increased. This indicated that the highest excited frequency resonance was mainly generated by the slot. Together with lower modes generated from stacked DRA, wideband DRA was formed.

C. NUMBER OF HOLES

Having optimized the antenna through the slot dimension, further bandwidth improvement was done by introducing holes in the resonators. By drilling a hole on the dielectric resonator, the electromagnetic field confined inside the DR are perturbed and the $Q-factor$ is degraded. The parametric studies on the number of holes inside the resonator was carried out and subsequently, its impedance bandwidth response was studied.

Fig. 6 shows the reflection coefficient of wideband hybrid DRA with different number of holes. It was found that by increasing the number of holes from 1 to 21, a slight upward shift in the frequency with an obvious enhancement in the impedance bandwidth were achieved. Significant increment on the antenna bandwidth is observed from 48.4% (without holes) to 75.8% (with holes) reflected the strength of the proposed method. According to (1), bandwidth enhancement can be explained from the volume reduction as the $Q-factor$ decreases. The presence of holes had introduced air permittivity inside the resonator structure, resulting in lower effective

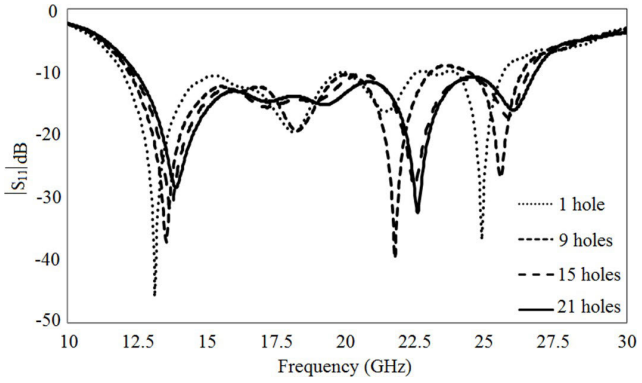

FIGURE 6. Simulated reflection coefficient of the wideband DRA with different number of holes.

permittivity of DR. Therefore, the whole frequency band shifted upward since the operational frequency is inversely proportional to the permittivity.

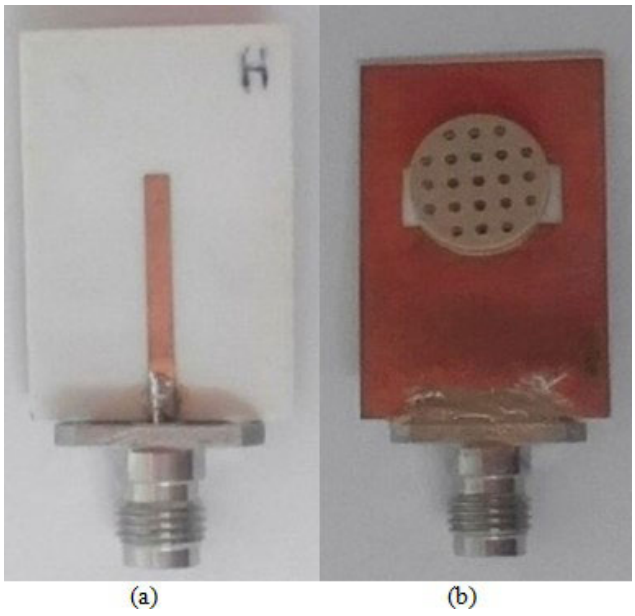

FIGURE 7. Fabricated hybrid stacked DRA (a) Back view (b) Front view.

IV. RESULTS AND DISCUSSIONS

From the conducted parametric studies, the optimal design parameters for the proposed DRA are listed in Table 3. A prototype of hybrid DRA as illustrated in Fig. 7 was later fabricated and tested to validate the simulation results experimentally. PNA-X Network Analyzer (N5245A) was used to measure the reflection coefficient. Radiation pattern characterization of the antenna was performed in an anechoic chamber.

Figure 8 shows the measured and simulated reflection coefficients of the proposed hybrid DRA. It can be observed that a good agreement between the simulation and measurement results were achieved. The simulated -10 dB return loss bandwidth ranging from 12.4 GHz to 26.7 GHz corresponded to a percentage bandwidth of approximately 73.1%. Whereas,

TABLE 3. Optimized parameters for the proposed design in mm.

L	W	La	Wa	S_1	S_2	R_{dr}	H_{d1}	H_{d2}	H_{d3}
30	20	13	5	0.5	2	5.5	0.813	1.6	1.27

L = length of dielectric substrate; S_2 = distance between two holes;
W = width of dielectric substrate; R_{dr} = radius of resonator;
L_a = slot length; H_{d1} = height of DR_1;
W_a = slot width; H_{d2} = height of DR_2;
S_1 = diameter of a hole; H_{d3} = height of DR_3.

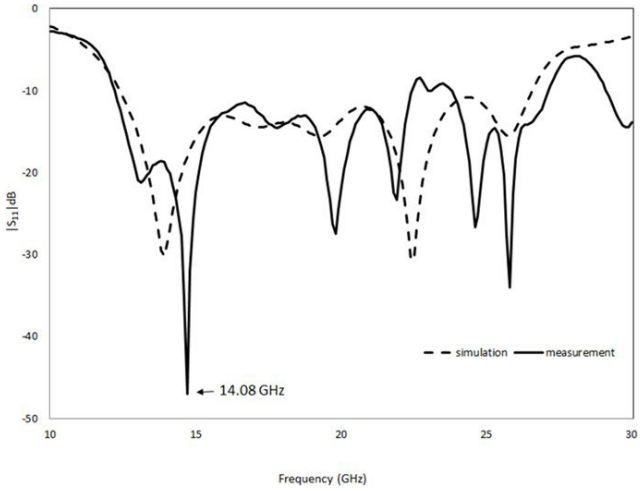

FIGURE 8. Simulated and measured reflection coefficients of the DRA.

the fabricated antenna promoted an impedance bandwidth of up to 75.8% (12.2 to 27.1 GHz), which shows an increment of about 2.7% in comparison with the simulation results. This difference in the simulated and measured impedance bandwidth attributes to the possible air-gaps remained present in the prototype of the proposed DRA. It can be clearly seen from Table 2 that the proposed antenna offered a wide impedance bandwidth as well as compact antenna structures by introducing air cavity inside the dielectric structure.

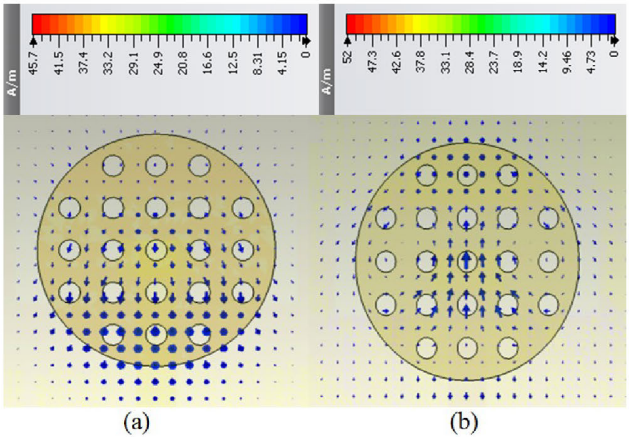

FIGURE 9. Electrical distribution of the resonant modes (a) 14.08 GHz, (b) 22.68 GHz.

Mode analysis on the wideband response of the DRA is presented in Figure 9 which shows the top view of the electrical field distribution at 14.08 GHz and 22.68 GHz.

With respect to the generated mode pattern, a wideband response of DRA was contributed by the multiple modes. All the resonances have a resonance pattern similar to that of the hybrid mode of HE but with variation in azimuth, radial and axial direction. The hybrid mode with the lowest resonance frequency of 14.08 GHz was HE_{11}. As frequency was increased to 22.68 GHz, the higher order mode of the HE_{12} became excited. As shown by Figure 9 (b), the two electric field loops on the face of resonator indicated an increment in radial variation. From the field visualization, it can be seen that the three layers stacked DRA operated as a whole resonator with different modes.

The measured far-field radiation patterns for the E and H planes at 13 GHz, 15 GHz and 18 GHz are illustrated in Figure 10. In the E-plane co-polarization, the pattern was observed from a top view where it is perpendicular to the z-axis, while for H-plane co-polarization, it was observed from the side view which is parallel to the z-axis. It can be observed that the radiation patterns were broadside in both the E and H-planes and the patterns were almost stable throughout the entire impedance bandwidth. The measured E-plane cross polarization level was approximately at least 50 dB lower as compared to the co-polarization at each frequency. On the other hand, the measured H-plane cross polarization level was approximately around 20-40 dB lower as compared to the co-polarization at each frequency. This shows that the proposed antenna received more power from the E-plane due to the huge differences in the co- and cross polarization levels in comparison to the H-plane. Moreover, the co- and cross polarization levels had also indicated that the proposed antenna was horizontally linearly polarized.

Figure 11 shows the measured directivity of the proposed antenna which was obtained using a gain transfer method where a standard gain horn antenna was used as a reference. A maximum measured directivity of 6.2 dBi was generated at 18 GHz with an average directivity of 5.65 dBi from the entire frequency range. Overall, the directivity of the proposed antenna was not showing much improvement even with the introduction of perforated structure since a single DRA normally has a low directivity of 5 dBi [31]. This can directly influence the aperture efficiency of the antenna which is defined by (13):

$$\alpha = \frac{\lambda^2 G}{4\pi} \tag{13}$$

where, G is the gain of the proposed antenna [32]. At 13 GHz, the aperture efficiency was achieved at only 37.4%. The percentage started to drop to 25.2% and 26.4% at 15 GHz and 18 GHz, respectively due to the effect of low gain level and shorter wavelength. Common directional antenna such as horn or array antennas can have an aperture efficiency of above 60% [33], [34].

It can also be noted that the gain was slightly dropping from 20 GHz to 25 GHz even though the reflection coefficient was good. A good reflection coefficient alone does not decide a better gain in an antenna since it is also dependent on its ability to radiate the received power. Some of the power input may be lost due to dielectric loss, as well as high frequency transmission. Thus, the total efficiency of

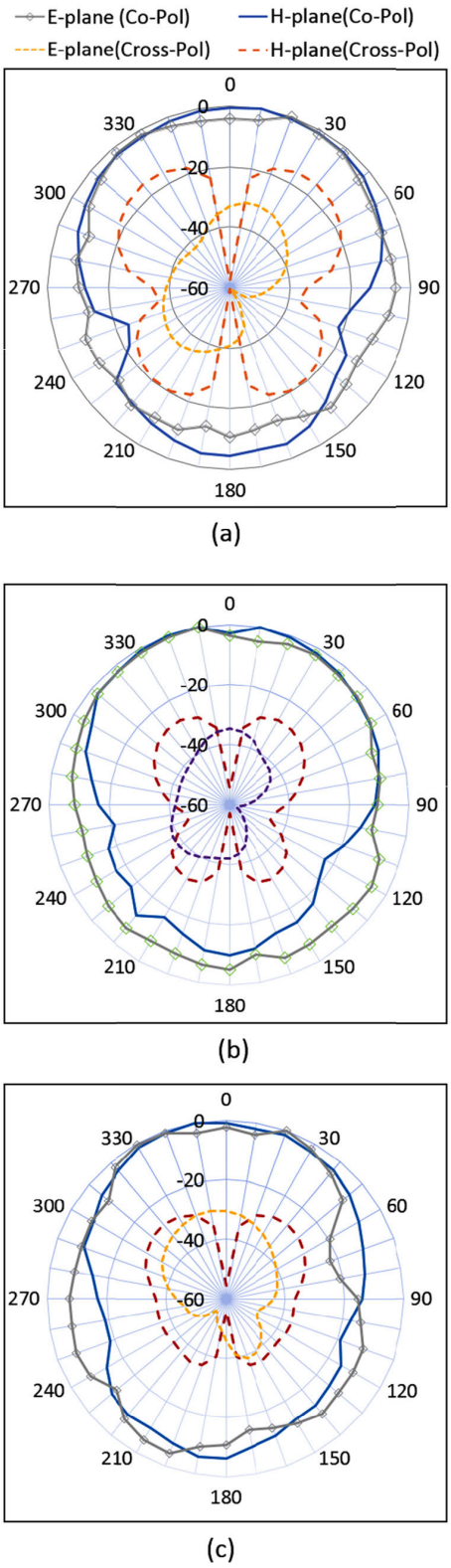

FIGURE 10. Radiation patterns in the E and H planes at (a) 13 GHz (b) 15 GHz and (c) 18 GHz.

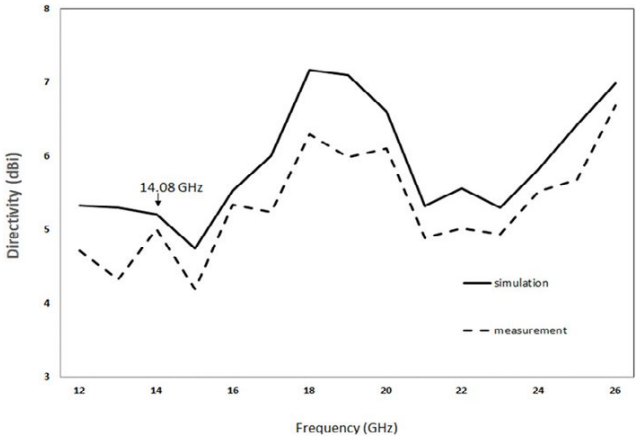

FIGURE 11. Simulated and measured directivity of the proposed hybrid DRA.

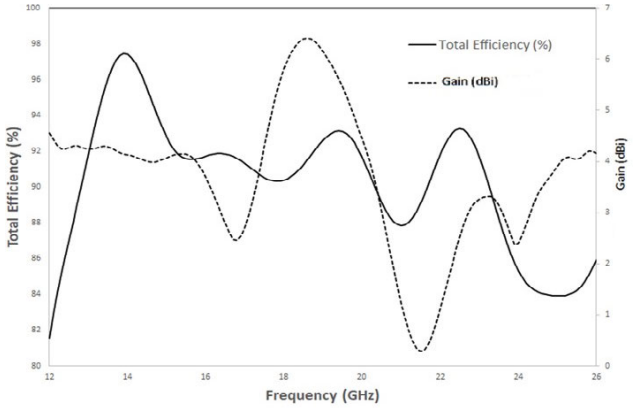

FIGURE 12. Total efficiency and gain of the proposed hybrid DRA.

the proposed antenna was investigated and is provided in Figure 12. It can be seen that the antenna efficiency decreased at higher frequency and the lowest efficiency occurred in between 24 GHz to 26 GHz. Another factor that contributes to a gain reduction is directivity. From Figure 12, it can be seen that the gain of the antenna decreased from 20 GHz to 25 GHz. The degradation of the gain was due to the broader coverage power received by the antenna. It can also be noted that the proposed antenna generated a very good return loss, S_{11} at 14 GHz but with a low gain value. Since, S_{11} only indicated the energy input accepted by the antenna in comparison to its reflected energy, there is no guarantee that all the accepted energy was being radiated to a specific location. At this particular frequency, the accepted energy fed to the proposed antenna was likely absorbed either into the dielectric substrate or dielectric resonator, thus reducing the radiated power and proportionally affecting the gain level.

V. CONCLUSION

In this study, a perforated stacked hybrid DRA made up of three multi-permittivity resonators and a resonating slot was designed and fabricated. These elements were merged and tightly stacked together to produce multiple modes and a wide operating bandwidth. A rectangular slot was used as the feeder which simultaneously acted as the radiator. The optimal arrangement of the three stacked DRs from bottom to top was in the order of ϵ_1 (3.38), ϵ_2 (4.55) and ϵ_3 (10.2). By introducing 21 identical circular holes inside the DRs, the bandwidth was significantly improved from 48.4% to 75.8% with an average directivity of 5.65 dBi. This hybrid DRA offers a significant feature of wide band characteristic while at the same time preserving its low-profile structure. Thus, from the combination of stacked DR and slot radiator with circular holes, a low-profile wideband hybrid stacked DRA can be designed and used for Ku and K bands application in the wideband communication systems.

REFERENCES

[1] S. Long, M. McAllister, and L. Shen, "The resonant cylindrical dielectric cavity antenna," *IEEE Trans. Antennas Propag.*, vol. 31, no. 3, pp. 406–412, May 1983.

[2] Q. Lai, G. Almpanis, C. Fumeaux, H. Benedickter, and R. Vahldieck, "Comparison of the radiation efficiency for the dielectric resonator antenna and the microstrip antenna at ka band," *IEEE Trans. Antennas Propag.*, vol. 56, no. 11, pp. 3589–3592, Nov. 2008.

[3] A. Petosa, *Dielectric Resonator Antenna Handbook*. Norwood, MA, USA: Artech House, 2007.

[4] W. Huang and A. A. Kishk, "Compact wideband multi-layer cylindrical dielectric resonator antennas," *IET Microw., Antennas Propag.*, vol. 1, no. 5, pp. 998–1005, Oct. 2007.

[5] G. Varshney, V. S. Pandey, R. S. Yaduvanshi, and L. Kumar, "Wide band circularly polarized dielectric resonator antenna with stair-shaped slot excitation," *IEEE Trans. Antennas Propag.*, vol. 65, no. 3, pp. 1380–1383, Mar. 2017.

[6] R. D. Gupta and M. S. Parihar, "Investigation of an asymmetrical E-shaped dielectric resonator antenna with wideband characteristics," *IET Microw., Antennas Propag.*, vol. 10, no. 12, pp. 1292–1297, Sep. 2016.

[7] S. M. Shum and K. M. Luk, "Characteristics of dielectric ring resonator antenna with an air gap," *Electron. Lett.*, vol. 30, no. 4, pp. 277–278, Feb. 1994.

[8] R. Chair, A. A. Kishk, and K. F. Lee, "Experimental investigation for wideband perforated dielectric resonator antenna," *Electron. Lett.*, vol. 42, no. 3, pp. 137–139, Jul. 2006.

[9] P. Patel, B. Mukherjee, and J. Mukherjee, "A compact wideband rectangular dielectric resonator antenna using perforations and edge grounding," *IEEE Antennas Wireless Propag. Lett.*, vol. 14, pp. 490–493, 2015.

[10] G. Massie, M. Caillet, M. Clenet, and Y. M. M. Antar, "A new wideband circularly polarized hybrid dielectric resonator antenna," *IEEE Antennas Wireless Propag. Lett.*, vol. 9, pp. 347–350, 2010.

[11] M. Zou and J. Pan, "Wideband hybrid circularly polarised rectangular dielectric resonator antenna excited by modified cross-slot," *Electron. Lett.*, vol. 50, no. 16, pp. 1123–1125, Jul. 2014.

[12] D. Guha, B. Gupta, and Y. M. M. Antar, "Hybrid monopole-DRAs using hemispherical/conical-shaped dielectric ring resonators: Improved ultrawideband designs," *IEEE Trans. Antennas Propag.*, vol. 60, no. 1, pp. 393–398, Jan. 2012.

[13] S. Fakhte, H. Oraizi, R. Karimian, and R. Fakhte, "A new wideband circularly polarized stair-shaped dielectric resonator antenna," *IEEE Trans. Antennas Propag.*, vol. 63, no. 4, pp. 1828–1832, Apr. 2015.

[14] A. Sharma and R. K. Gangwar, "Circularly polarised hybrid Z-shaped cylindrical dielectric resonator antenna for multiband applications," *IET Microw., Antennas Propag.*, vol. 10, no. 12, pp. 1259–1267, Sep. 2016.

[15] A. Azari, A. Ismail, A. Sali, and F. Hashim, "A new super wideband fractal monopole-dielectric resonator antenna," *IEEE Antennas Wireless Propag. Lett.*, vol. 12, pp. 1014–1016, 2013.

[16] A. Sharma, G. Das, and R. K. Gangwar, "Design and analysis of tri-band dual-port dielectric resonator based hybrid antenna for WLAN/WiMAX applications," *IET Microw., Antennas Propag.*, vol. 12, no. 6, pp. 986–992, May 2018.

[17] G. Das, A. Sharma, and R. K. Gangwar, "Wideband self-complementary hybrid ring dielectric resonator antenna for MIMO applications," *IET Microw., Antennas Propag.*, vol. 12, no. 1, pp. 108–114, Jan. 2018.

[18] Y.-H. Qian and Q.-X. Chu, "A broadband hybrid monopole-dielectric resonator water antenna," *IEEE Antennas Wireless Propag. Lett.*, vol. 16, pp. 360–363, 2017.
[19] R. K. Chaudhary, K. V. Srivastava, and A. Biswas, "Wideband multi-layer multi-permittivity half-split cylindrical dielectric resonator antenna," *Microw. Opt. Technol. Lett.*, vol. 54, no. 11, pp. 2587–2590, Nov. 2012.
[20] R. K. Chaudhary, K. V. Srivastava, and A. Biswas, "Three-element multilayer multipermittivity cylindrical dielectric resonator antenna for wideband applications with omnidirectional radiation pattern and low cross-polarization," *Microw. Opt. Technol. Lett.*, vol. 54, no. 9, pp. 2011–2016, Sep. 2012.
[21] R. K. Chaudhary, K. V. Srivastava, and A. Biswas, "Broadband four-element multi-layer multi-permittivity cylindrical dielectric resonator antenna," *Microw. Opt. Technol. Lett.*, vol. 55, no. 4, pp. 932–937, Apr. 2013.
[22] P. Patel, B. Mukherjee, and J. Mukherjee, "A compact wideband rectangular dielectric resonator antenna using perforations and edge grounding," *IEEE Antennas Wireless Propag. Lett.*, vol. 14, pp. 490–493, 2014.
[23] H. Zhang, D.-B. Yan, and N.-C. Yuan, "Microstrip dipole antenna with H-shaped coupling aperture," in *Proc. Asia–Pacific Microw. Conf. (APMC)*, 2005, pp. 1–2.
[24] R. Chair, A. A. Kishk, K. F. Lee, C. E. Smith, and D. Kajfez, "Microstrip line and CPW fed ultra wideband slot antennas with U-shaped tuning stub and reflector," *Prog. Electromagn. Res. PIER*, vol. 56, pp. 163–182, 2006, doi: 10.2528/PIER05060701.
[25] Z. Aijaz and S. C. Shrivastava, "Effect of the different shapes aperture coupled microstrip slot antenna," *Int. J. Electron. Eng.*, vol. 2, no. 1, pp. 103–105, 2010.
[26] Z. Aijaz and S. C. Shrivastava, "An introduction of aperture coupled microstrip slot antenna," *Int. J. Eng. Sci. Technol.*, vol. 2, no. 1, pp. 36–39, 2010.
[27] G. D. Makwana and D. Ghodgaonkar, "Wideband stacked rectangular dielectric resonator antenna at 5.2 GHz," *Int. J. Electromagn. Appl.*, vol. 2, no. 3, pp. 41–45, Aug. 2012.
[28] P. Rezaei, M. Hakkak, and K. Forooraghi, "Design of wide-band dielectric resonator antenna with a two-segment structure," *Prog. Electromagn. Res.*, vol. 66, pp. 111–124, 2006, doi: 10.2528/PIER06110701.
[29] A. Petosa and A. Ittipiboon, "Design and performance of a perforated dielectric Fresnel lens," *IEE Proc.—Microw., Antennas Propag.*, vol. 150, no. 5, pp. 309–314, Oct. 2003.
[30] A. Petosa, N. Simons, R. Siushansian, A. Ittipiboon, and M. Cuhaci, "Design and analysis of multisegment dielectric resonator antennas," *IEEE Trans. Antennas Propag.*, vol. 48, no. 5, pp. 738–742, May 2000.
[31] T. Elkarkraoui, G. Y. Delisle, N. Hakem, and Y. Coulibaly, "New hybrid design for a broadband high gain 60-GHz Dielectric Resonator Antenna," in *Proc. 7th Eur. Conf. Antennas Propag. (EuCAP)*, Apr. 2013, pp. 2444–2447.
[32] W. L. Stutzman and G. A. Thiele, *Antenna Theory and Design*, 3rd ed. Hoboken, NJ, USA: Wiley, 2012.
[33] J. Guo, S. Liao, Q. Xue, and S. Xiao, "Planar aperture antenna with high gain and high aperture efficiency for 60-GHz applications," *IEEE Trans. Antennas Propag.*, vol. 65, no. 12, pp. 6262–6273, Dec. 2017.
[34] S. Azodolmolky, J. Perello, M. Angelou, F. Agraz, L. Velasco, S. Spadaro, Y. Pointurier, A. Francescon, C. V. Saradhi, P. Kokkinos, E. Varvarigos, S. A. Zahr, M. Gagnaire, M. Gunkel, D. Klonidis, and I. Tomkos, "Experimental demonstration of an impairment aware network planning and operation tool for Transparent/Translucent optical networks," *J. Lightw. Technol.*, vol. 29, no. 4, pp. 439–448, Feb. 2011.

IHSAN AHMAD ZUBIR was born in Perak, Malaysia, in 1985. He received the B.Eng. degree in electrical and electronics engineering from Universiti Malaysia Pahang, Malaysia, in 2008, and the M.Sc. and Ph.D. degrees in electrical and electronics engineering from Universiti Sains Malaysia, Malaysia, in 2012 and 2018, respectively. He is currently working as a Senior RF Designer at Sapura Secured Technologies Sdn Bhd, Malaysia. His research interests include dielectric resonator antenna, wireless transceiver, and RF circuits design.

MOHAMADARIFF OTHMAN received the bachelor's degree in electronic engineering from Multimedia University, Malaysia, in 2006, and the M.Sc. degree in RF and microwave field and the Ph.D. degree in antenna and propagation from Universiti Sains Malaysia (USM), Malaysia, in 2008 and 2015, respectively. He joined the Department of Electrical Engineering, University of Malaya, Malaysia, as a Senior Lecturer, in 2016, after serving a private university for almost one and half year. His research interests include 5G antenna, dielectric characterization, dielectric resonator antenna design, and optimization of antenna design.

UBAID ULLAH (Member, IEEE) received the B.S. degree in electrical engineering from the CECOS University of IT and Emerging Sciences, Pakistan, in 2010, and the M.S. and Ph.D. degrees in electronic engineering from Universiti Sains Malaysia, Malaysia, in 2012 and 2017, respectively. He was a Postdoctoral Researcher with the School of Science and Engineering, Reykjavik University, Iceland. He has published several papers in ISI indexed journals and some well-reputed international conferences. His current research interests include dielectric resonator antennas (DRAs), wideband DRAs, microwave circuits, low-temperature-cofired-ceramics-based antenna in package, applied electromagnetics, and small antennas.

SHAHANAWAZ KAMAL was born in Mumbai, India. He received the B.E. and M.E. degrees in electronics and telecommunication engineering from the University of Mumbai, India, in 2013 and 2017, respectively. He is currently pursuing the Ph.D. degree in antenna and propagation with the School of Electrical and Electronic Engineering, Universiti Sains Malaysia, Malaysia. He joined Vedang Cellular Services Pvt., Ltd., India, as an In-Building Solution (IBS) Engineer, in 2014. He was a Visiting Lecturer with the Department of Information Technology, M. H. Saboo Siddik Polytechnic, India, in 2016. His research interests include conceptualization, design, development, and measurement of PCB or sheet metal antennas with single element, array and MIMO configurations for ISM, LTE, mmWave, and 5G applications.

MOHD FARIZ AB RAHMAN was born in Kota Bharu, Malaysia. He received the B.Eng. degree (Hons.) in materials engineering from Universiti Malaysia Perlis, Malaysia, in 2010, and the M.Sc. and Ph.D. degrees in materials engineering from Universiti Sains Malaysia (USM), Malaysia, in 2014 and 2017, respectively. In 2018, he joined the School of Electrical and Electronic Engineering, USM, as a Research Assistant, under the supervision of Prof. Ir. Dr. Mohd Fadzil Bin Ain. He has authored or coauthored more than 20 articles. His research interests include materials engineering, materials science, and electro-ceramics which include the development of ceramic materials for electronic devices.

ROSLINA HUSSIN received the B.Sc. degree in electrical engineering from the University of Tulsa, Oklahoma, USA, in 1994, and the M.Sc. degree in communication engineering from Universiti Sains Malaysia (USM), in 2016, where she is currently pursuing the Ph.D. degree in antenna and propagation with the School of Electrical and Electronic Engineering. She works as a Research Officer with the School of Electrical Electronic, USM. Her research interests include RF and microwave systems, wave propagation, and engineering studies.

MOHAMAD FAIZ BIN MOHAMED OMAR received the B.Eng. degree (Hons.) in electronic engineering and the M.Sc. degree in RF microwave engineering from Universiti Sains Malaysia, Nibong Tebal, in June 2014 and 2017, respectively. He is currently a Research Officer with the Collaborative Microelectronic Design Excellence Centre (CEDEC), Universiti Sains Malaysia. His current research interests include simulation and design of high RF and high-power devices, microwave tomography, and digital image processing.

ABDULLAHI S. B. MOHAMMED received the B.Eng. degree in electrical engineering from Bayero University Kano, Nigeria, in 2008, and the M.Sc. degree in electrical engineering with a prime focus on telecommunication from Ahmadu Bello University, Nigeria, in 2014. He is currently pursuing the Ph.D. degree in antenna and propagation with the School of Electrical and Electronic Engineering, Universiti Sains Malaysia, Malaysia.

MOHD FADZIL BIN AIN received the B.S. degree in electronic engineering from Universiti Teknologi Malaysia, Malaysia, in 1997, the M.S. degree in radio frequency and microwave from Universiti Sains Malaysia (USM), Malaysia, in 1999, and the Ph.D. degree in radio frequency and microwave from the University of Birmingham, U.K., in 2003. In 2003, he joined the School of Electrical and Electronic Engineering, USM. He is currently a Professor with VK7 grade, the Dean of Research, Postgraduate and Networking, and the Director of Collaborative Microelectronic Design Excellence Centre (CEDEC). He is actively involved in technical consultancy with several companies in repairing microwave equipment. His current research interests include MIMO wireless system on FPGA/DSP, Ka-band transceiver design, dielectric antenna, RF characterization of dielectric material, and microwave propagation study. His awards and honors include International Invention Innovation Industrial Design and Technology Exhibition, International Exposition of Research and Inventions of Institutions of Higher Leaning, Malaysia Technology Expo, Malaysian Association of Research Scientists, Seoul International Invention Fair, iENA, Best Paper for the 7th WSEAS International Conference on Data Networks, Communications, Computers, and International Conference on X-Ray and Related Techniques in Research and Industry.

ZAINAL ARIFIN AHMAD received the B.S. degree in materials engineering from Universiti Sains Malaysia, Malaysia, the M.S. degree from the Institute of Science and Technology, The University of Manchester, U.K., and the Ph.D. degree from the University of Sheffield, U.K. He is currently a Senior Professor with the School of Materials and Mineral Resources Engineering, Universiti Sains Malaysia. His current research interests include ZTA ceramic for cutting insert, low-temperature-cofired-ceramics-based circuits, metal–ceramic joining, crystal glaze ceramic, TCP bioceramic, and dielectric ceramic for antennas.

MOHD ZAID ABDULLAH (Member, IEEE) received the B.App.Sc. degree in electronics from Universiti Sains Malaysia (USM), Nibong Tebal, Malaysia, in 1986, and the M.Sc. degree in instrument design and application and the Ph.D. degree from the Institute of Science and Technology, The University of Manchester, Manchester, U.K., in 1989 and 1993, respectively. He worked as a Test Engineer with Hitachi Semiconductor, Malaysia. He was carrying out research in Electrical Impedance Tomography with the Institute of Science and Technology, The University of Manchester. He is currently a Lecturer and a Professor with the School of Electrical and Electronic Engineering, USM. His research interests include microwave tomography, digital image processing, computer vision, and ultra-wide band sensing. He has published numerous research papers in international journals and conference proceedings. His one of the papers was awarded the Senior Moulton Medal for the best article published by the Institute of Chemical Engineering, in 2002.